RESEARCH ARTICLE

Accurate Indoor Positioning for UWB-Based Personal Devices Using Deep Learning

SANGMO SUNG, **HOKEUN KIM**, **AND JAE-IL JUNG**, (Member, IEEE)

Department of Electronic Engineering, Hanyang University, Seoul 04763, South Korea

Corresponding authors: Hokeun Kim (hokeun@hanyang.ac.kr) and Jae-Il Jung (jijung@hanyang.ac.kr)

ABSTRACT Recently, there has been a rapidly emerging demand for localization technologies to provide various location-based services in indoor environments, such as smart buildings, smart factories, and parking lots, as well as outdoor environments. Ultra-wideband (UWB), an emerging wireless technology, provides opportunities for precise indoor positioning with sub-meter accuracy, much more accurate than WiFi or BLE-based techniques, thanks to its signal and communication characteristics. UWB technology has recently begun to be applied to personal devices such as smartphones and is expected to be used for indoor localization of personal devices. However, personal devices often cause signal problems because they are worn on human hands or bodies and move dynamically or are in a non-line-of-sight (NLoS) condition, such as pockets or bags. Therefore, these challenges in the dynamic environment of personal devices must be addressed to enable accurate indoor positioning services based on UWB. In this paper, we propose a novel UWB-based indoor positioning approach that significantly improves localization accuracy under dynamic personal device environments. Our proposed approach detects various NLoS conditions of personal environments by leveraging channel impulse response (CIR) and deep learning. Based on the detected NLoS conditions, the proposed approach adjusts the Kalman filter to adaptively estimate the position of the target UWB-based personal device. Specifically, the distance measurement errors by NLoS are minimized by applying weights determined by deep learning to the Kalman filter. Through experiments conducted in practical indoor environments, we have shown that our proposed approach considerably improves the accuracy compared to the traditional Kalman filter-based and trilateration approaches. According to our method of counting the number of points relative to ground truth, the proposed positioning system improved positioning accuracy significantly by 20.84% to 27.22% with an error tolerance of ±25 cm and by 7.78% to 22.78% with an error tolerance of ±50 cm, compared to the traditional approaches.

INDEX TERMS UWB, personal device, indoor localization, TWR, ranging error compensation, deep learning, LoS & NLoS classification, trilateration positioning algorithm, weight adaptive Kalman filter.

I. INTRODUCTION

Various location-based technologies for indoor environments have been emerging in response to the demand for *indoor localization services*. There is a particularly high demand for high-precision indoor localization across industries [1]. This demand leads to the evolution of various applications

The associate editor coordinating the review of this manuscript and approving it for publication was Barbara Masini.

for location-based services delivered in indoor environments, including buildings, department stores, airports, and museums.

However, due to the limitations of conventional localization methodology based on (1) *wireless communication* [2], [3], [4], [5], [6] or (2) *various sensor techniques* [7], [8], [9], it has been difficult for the traditional approaches to meet the high-precision requirements of applications, such as navigation and robot positioning [10].

Wireless communication technologies such as WiFi and Bluetooth low energy (BLE) calculate locations leveraging the received signal strength indicator (RSSI). However, RSSI tends to fluctuate due to environmental obstacles such as multipath fading, refraction, diffraction, and interference by devices using similar frequency bands [11], [12], [13], [14], [15]. As a result, positioning accuracy by inaccurate RSSI is difficult to trust.

In addition, positioning based on sensors, such as vision and inertial measurement unit (IMU) sensors, makes it challenging to achieve positioning with stable accuracy because of the physical limitations of the sensor in certain environments. Several sensor fusion techniques and data filtering techniques for indoor position tracking have been studied to overcome these accuracy degradation problems [7], [8].

However, as sensor fusion technology requires multiple sensors, processing large amounts of sensor data increases hardware costs and computation time for filtering the data, which delays the positioning refresh cycle significantly.

The *ultra-wideband (UWB) technology* is now viewed as a game changer to overcome the aforementioned challenges [16]. Following this trend, personal device manufacturers are starting to include UWB capability in their personal devices by default because of the technological advantages of UWB. Leading smartphone manufacturers such as Google, Apple, and Samsung have launched their flagship smartphones with built-in UWB chipsets [17]. Also, recently, Apple and Samsung started developing their own UWB chips.

UWB uses ultra-wideband frequencies; thus, UWB has the advantage of being resistant to interference with other communications thanks to its wide bandwidth, having a fading margin, and a high multi-path diversity gain [17]. UWB can also provide a more accurate and stable positioning technology compared to RSSI-based positioning methods [18], which are heavily affected by radio signal attenuation due to obstacles, multipath fading, and signal interference because UWB uses the time-of-flight (ToF) method for ranging or positioning.

UWB positioning methods are roughly threefold; (1) trilateration, (2) multilateration, and (3) angle-of-arrival (AoA). The trilateration determines the position based on the distance measured between the devices using a radius of the circle (or sphere) from each device. The multilateration is similar to trilateration except that it uses hyperbolas (in 2D cases) or hyperboloids (in 3D cases) using TDoA (time difference of arrival) instead of circles or spheres using ToA (time of arrival). AoA positioning uses the distance data and the phase angle of the arrival signal [16], [19]. In all three methods, distance data calculated through the signal transfer time between equipment is an important factor in determining the accuracy of the positioning [20].

Personal device location tracking using UWB is potentially highly accurate compared to location tracking using other wireless communications and does not require a separate device.

However, when the UWB terminal dynamically moves, because the direct propagation path of the UWB signal can be obstructed, the additional delay will occur in the ToF, resulting in biased range measurements. The dynamic circumstances around UWB devices render high-precision ranging challenging [21].

For example, personal devices, such as mobile phones, move dynamically with the user in hand, resulting in incorrect ToF calculations by indirect path signals due to the lack of a direct path of UWB signal propagation by unpredictable obstacles, which can lead to ranging errors and potentially positioning errors [21].

Ranging errors are particularly noticeable in channel environments where line-of-sight (LoS) is not secured [22], [23], such as inside pockets and bags.

To address the challenges with the personal device environments, we propose an indoor positioning scheme using a novel ranging error correction technique for high-accuracy indoor positioning systems for personal devices such as mobile phones. The key idea of our approach is to estimate the reliability of UWB ranging using channel impulse response (CIR) through deep learning.

We use the Kalman filter to reduce errors in distance data with the filter parameters based on CIR-based ranging measurements to improve correction efficiency. Based on the estimated reliability of the measured distance values through deep learning, we determine the estimates of the distance values by adjusting the weights for the measurement of the measurement model and the prediction of the system model of the Kalman filter.

The main contributions of our approach are as follows:
- We propose novel deep learning-based UWB two-way ranging (TWR) error correction algorithms for the high-accuracy localization of personal devices as UWB tags. (Section III)
- We propose an optimal Kalman gain calculation logic for the Kalman filter along with a non-line-of-sight (NLoS) probability calculation model based on UWB CIR using deep learning. (Section III-C)
- The proposed optimal model for Kalman gain and the logic for NLoS probability can readily incorporate dynamic ranging errors and can be applied to UWB localization algorithms.
- Through realistic experiments, our approach significantly improves the localization accuracy by 20.84% to 27.22% with an error tolerance of B125 cm and by 7.78% to 22.78% with an error tolerance of B150 cm, compared to the traditional Kalman filter and trilateration-based approaches. (Section IV-C)

The rest of this paper is organized as follows: Section II presents a literature review of existing research on UWB-based ranging. In Section III, we propose a novel approach for distance error compensation in personal device positioning environments. Section IV evaluates the performance of the proposed approach. Section V concludes the paper.
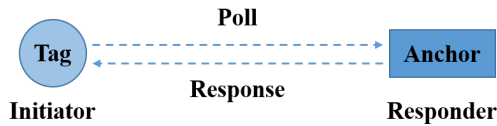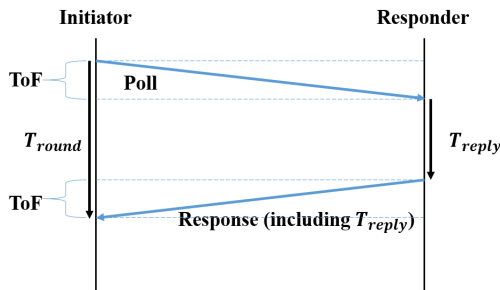
FIGURE 1. Message exchange in Single-sided TWR.

FIGURE 2. Process of UWB Single-sided TWR.

II. RELATED WORK

Since the advent of UWB wireless communication technology, recent advancements in research on indoor positioning systems using UWB have drawn considerable interest from researchers. In particular, in UWB TWR-based trilateration positioning, one of the main research streams has been a technique for correcting ranging errors to enable high-precision position estimation in an indoor environment.

This section reviews the study of distance measurement techniques using UWB, line-of-sight (LoS) and non-line-of-sight (NLoS) classification studies using UWB channel impulse response (CIR), error correction of distance data measured by TWR between two UWB nodes, and UWB-based localization accuracy improvement studies using deep learning.

A. UWB-BASED RANGING METHOD

Because the UWB characteristic is robust in multipath and has a short pulse width, it has a high resolution, which enables precise measurement of time-of-flight (ToF). UWB uses TWR technology to calculate distance based on ToF. TWR is commonly used to measure the distance between two wireless transceiver nodes.

Although UWB can accurately measure ToF, but still contains errors. Techniques for correcting errors for more accurate positioning have been studied [24], [25], [26].

FIGURE 1 provides a brief description of the single-sided TWR (SS-TWR) method, one of the representative TWR methods. SS-TWR is a method of ranging through one message exchange between the *initiator* and the *responder*. FIGURE 2 illustrates the specific UWB SS-TWR process. In SS-TWR, the initiator obtains information about T_{reply} from the response message received from the responder. You can then calculate ToF, which is half the difference between the two, from the known T_{round} and T_{reply}. This method is less accurate than other improved TWR methods but is often used because it is suitable for low-performance embedded systems due to low computation.
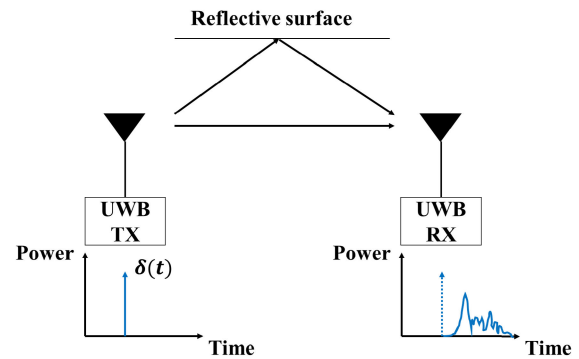

FIGURE 3. NLoS components included in the received UWB signals.

Among other improved TWR methods, Sidorenko et al. [27] studied message exchange procedures in TWR in other ways: asymmetric double-sided two-way ranging (ADS-TWR), alternative double-sided TWR (AltDS-TWR), and symmetrical double-sided TWR (SDS-TWR), which demonstrate the effect of smaller ranging measurement errors compared to commonly used SS-TWR methods [28], [29]. However, the complexity of the message exchange method itself increases the channel resources required for ranging, and there is still a problem that ranging speed is greatly reduced in communication between multiple nodes.

B. LoS, NLoS CLASSIFICATION METHODS USING UWB CIR

In the field of wireless communication technology, research has been actively conducted for channel state estimation through transmission and reception signals. In particular, since the UWB transmission signal is ideally close to the pulse signal, it is possible to estimate the channel status with the received signal because the received signal reflects most of the channel status.

Propagation signals are divided into the direct path through the shortest path and multipath through diffraction, refraction, reflection, etc. Naturally, multipath signals take longer to reach the receiver than the direct path signal. Thus, multipath signals tend to be further attenuated in terms of power while the signal is propagated, as shown in FIGURE 3, making it more difficult for the receiver to sense the reception time and reception strength of the signal.

In order to distinguish the direct path signal and indirect path signals, it is necessary to determine whether the received signals include multipath signals generated under NLoS conditions [30], [31]. Channel impulse response (CIR) is a representative indicator for distinguishing the direct path signal and indirect path signals in UWB communication as illustrated in FIGURES 4 and 5.

The CIR data indicate the characteristics of the channel, such as skewness, kurtosis, and location of samples with the maximum size and the average over-delay, which allows reasonable classification of data with nonlinear features [32], [33], [34], [35].

Below we illustrate the formula for obtaining the indicators of the CIR reflecting the channel characteristics. The received
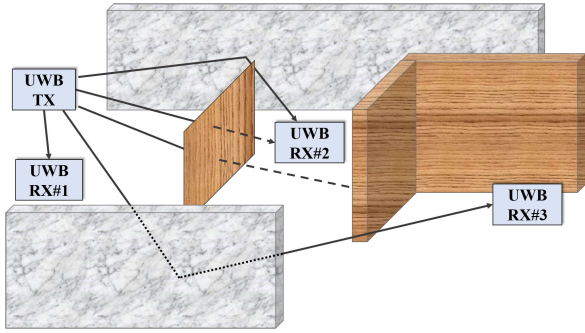
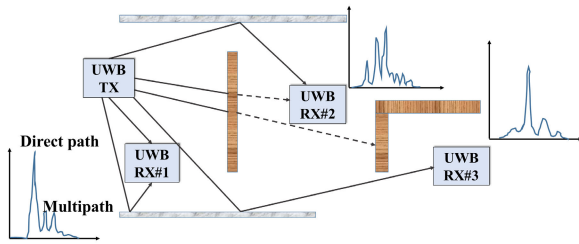**FIGURE 4.** Received UWB signals via various paths.

FIGURE 5. Top view of received channel impulse responses of various paths in UWB TWR shown in FIGURE 4.

signal from the UWB is formulated as follows:

$$r(t) = s(t) * h(\tau; t) + n(t) \tag{1}$$

The energy of the received signal is as follows:

$$E = \int_{-\infty}^{\infty} |r(t)|^2 dt \tag{2}$$

The maximum amplitude of the received signal is as follows:

$$r_{max} = \max r(t) \tag{3}$$

The index of the maximal amplitude in the CIR represents rise time:

$$T_{rise} = \arg\min_t c_{max} \tag{4}$$

The Mean excess delay is as follows:

$$\tau_m = \frac{\int_{-\infty}^{\infty} t|c(t)|^2 dt}{E} \tag{5}$$

Kurtosis:

$$\kappa = \frac{E[(|c(t)| - \mu)^4]}{\sigma^4} \tag{6}$$

Skewness:

$$\gamma = \frac{E[(|c(t)| - \mu)^3]}{\sigma^3} \tag{7}$$

We utilized the amplitude data of CIR of the received signals as they are most commonly used for LoS and NLoS classification.

C. MITIGATION OF UWB TWO-WAY RANGING MEASUREMENT ERROR

Various studies have been conducted to mitigate the errors contained in the TWR measurement data of the UWB. The TWR measurement data includes errors due to the environment being measured, the device's own fault, etc.

In particular, since errors according to the measurement environment are inevitable errors that occur outside the device, many studies are being conducted to classify environments that contain many errors as a way to solve this problem. Among them, when calculating TWR using UWB, studies are active to reduce the ranging error using an indicator called CIR that can identify channel states.

Channel impulse response (CIR) signals are used directly to extract high semantic features to estimate LoS or NLoS conditions [36]. Among several attempts to classify the environment by analyzing CIR, a prominent approach in recent studies is the use of artificial intelligence.

Wymeersch et al. [25] proposed a machine learning-based ranging error mitigation technique. This is a strategy that combines information about constraints on ranging errors with SVM or regression techniques and significantly improves performance over traditional approaches. Yu et al. [37] proposed ways to identify and scope NLoS based on low environmental dependence and prior knowledge independent fuzzy comprehensive evaluation. Kim et al. [38]. proposed a method to estimate the error values included in UWB TWR measurements based on channel conditions through the LSTM model and correct them through EKF.

D. UWB-BASED POSITIONING METHOD
In the latest UWB standard, the IEEE 802.15.4z standard, the ranging method introduces TWR, OWR (one-way ranging) for TDoA localization, as the recommended ranging technology used by devices applying the IEEE 802.15.4/4z standard [39]. The use cases of UWB technology can be extended to the localization of tags through this ranging technology. This section briefly describes the two typical methods of recommended localization technology.

1) OWR-BASED MULTILATERATION POSITIONING METHOD
The tag periodically sends a Blink signal to the anchor. Because each anchor is at a different distance from the tag, the tag transmits a signal and arrives at all anchors at different times. The difference in the time the signal arrives at the two anchors can be used to calculate hyperbolic [40], [41], [42], [43].

At least three hyperbolic intersect to provide the location of the tag. This method does not require tags to be synchronized with anchors, but anchors must be synchronized with each other. The accuracy of this synchronization has a significant impact on location accuracy [44].

FIGURE 6 shows a conceptual diagram of an OWR-based multilateration consisting of four anchors.
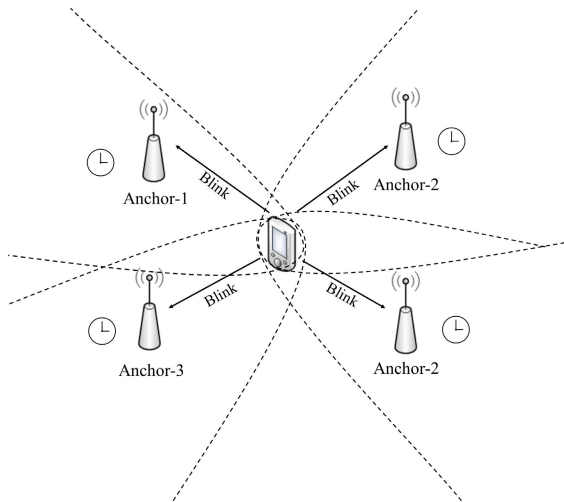
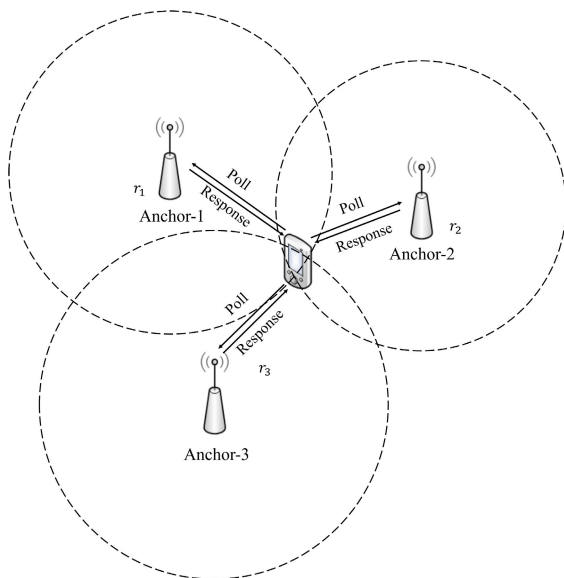**FIGURE 6.** UWB OWR-based multilateration Positioning.

FIGURE 7. UWB TWR-based trilateration Positioning.

2) TWR-BASED TRILATERATION POSITIONING METHOD

The TWR-based trilateration positioning scheme is neither complicated nor requires time synchronization between anchors compared to the OWR-based method. This means that configuring the positioning infrastructure can be simpler [40], [45]. Because the location is calculated through TWR, distance data using the propagation time of UWB signals inevitably contain errors due to errors in signal arrival time by multipath [18], [46], [47]. Therefore, achieving high positioning accuracy requires mitigating errors in TWR measurements. For example, the approach proposed in this paper uses distance and UWB CIR analysis to mitigate and correct measurement errors. FIGURE 7 shows a conceptual diagram of a TWR-based trilateration.

E. UWB POSITIONING ACCURACY IMPROVEMENT BASED ON ARTIFICIAL INTELLIGENCE

The accuracy of UWB TWR-based trilateration positioning techniques can be improved by modifying trilateration positioning algorithms or directly ranging error mitigation techniques at the physical layer to minimize the ranging error.

Kalman filter (KF), used in existing ranging error mitigation techniques [48] and localization algorithms, have received widespread attention because they are classical methods for state estimation of dynamic systems [49], [50], [51]. However, this uses a fixed noise covariance matrix, making it difficult to reflect all the changing noise in a dynamic positioning environment. To address this problem, ranging error mitigation techniques using machine learning [25] and deep learning have recently been studied. There are also studies of applying deep learning directly to localization algorithms [52].

However, in previous studies, deep learning-based ranging error mitigation techniques were studied in simulation level [48] or required accurate LoS, NLoS classification because they corrected ranging errors through binary classification for LoS, NLoS. In addition, modifications to deep learning-based localization algorithms require extensive data collection and a lot of data processing time, as models must be learned and used based on different types of data, such as ranging measurement, CIR, TDoA, and RSSI.

In this study, UWB CIR ranging measurements are used to obtain deep learning-based NLoS probabilities and use them to determine the size of the noise matrix of the Kalman filter to immediately mitigate ranging errors that vary in real-time. In addition, by using the learning data limited to ranging measurements and CIR, the collection of learning data required for deep learning model learning can be simplified, and data processing time can be drastically reduced.

III. PROPOSED APPROACH FOR UWB-BASED PERSONAL DEVICE POSITIONING

The indoor positioning accuracy of a personal device such as a mobile phone using UWB changes its pose (e.g., angles) and position dynamically depending on the characteristics of the personal device being tagged, so the direction of the antenna and the presence or absence of obstacles to propagation vary from time to time. The effects of these characteristics of personal devices behave the same as an obstacle to accurate positioning. Therefore, UWB-based indoor positioning systems on personal devices require steps to minimize contextual distance errors and minimize errors in calculated positions.

However, dynamically changing postures and environments make it difficult to predict all errors that occur. We have developed a new indoor location estimation technique for mobile phones based on deep learning to flexibly consider their pose and environment. UWB data measured in different environments can be used to classify the positioning environment and to update the parameters of the Kalman filter for specific environments to improve accuracy for distance predictions.

Our proposed indoor positioning system for personal devices consists of three main elements.

- **Element 1**: Deep learning-based propagation environment classifier

TABLE 1. Abbreviations and acronyms.

Abbreviation	Expansion
CIR	Channel impulse response
ToF	Time of flight
LoS	Line of sight
NLoS	Non LoS
DNN	Deep neural network
OWR	One-way ranging
TWR	Two-way ranging
SS-TWR	Single sided TWR
ADS-TWR	Asymmetric double sided TWR
AltDS-TWR	Alternative double sided TWR
SDS-TWR	Symmetrical double sided TWR
KF	Kalman filter
WAKF	Weighted adaptive KF

- **Element 2**: Kalman filter-based ranging measurement error correction algorithm
- **Element 3**: Trilateration positioning algorithm

This section describes the abbreviated list, the overall system structure, the proposed deep learning-based classification model, Kalman filter-based distance error correction, and trilateration positioning algorithms.

Before diving into the discussion on our proposed approach, we provide a list of abbreviations used to improve the readability of the paper is shown in TABLE 1, to be used throughout the rest of the paper because many abbreviations are used in the field of UWB, positioning, and deep learning.

A. SYSTEM ARCHITECTURE

We propose a novel Kalman filter-based TWR error correction system for mobile phone positioning to take into account the environmental factors between UWB tags and anchors that affect positioning results. The ultimate purpose of this system is to increase the accuracy of location tracking with UWB CIR information when mobile phone positioning is disadvantageous. UWB CIR is used as a key indicator for classifying situations in which the location of UWB mobile phones is disadvantageous. Here, to increase the accuracy of CIR-based LoS and NLoS classification, we obtain data by further segmenting NLoS situations rather than binary classification.

It takes advantage of the fact that the correlation between the measured CIR values in the NLoS situation is higher than in the LoS situation and that the NLoS situation in the personal device can be determined by several typical situations with high probability. Therefore, the model's contextual classification ability is also enhanced by learning deep learning models by collecting data that can further specify the NLoS situation. For example, NLoS due to pockets is more similar to NLoS for bags and humans than to LoS. This can provide more evidence for classifiers to distinguish between NLoS situations.

FIGURE 8 shows the proposed overall system structure. In the first environment to obtain data, we assume that the mobile phone positioning environment is divided into three cases - two NLoS cases (Cases 1 and 2 in FIGURE 8) and one LoS case (Case 3 in FIGURE 8). First, we obtained data for **Case 1**: when a personal device is in a pocket and **Case 2**: when a personal device is in a pocket. In addition, we obtained data under LoS (**Case 3**) by assuming the situation personal device in an open space.

Since the proportion of learning data is ultimately an important factor in determining the classification propensity of deep learning models, we obtain similar amounts in all three cases. We performed experiments on the test environment with the tag in the pocket, bag, or hand in ranging situations between the anchor and the tag. The UWB data used for learning consists of 1016 CIR and distance measurements and labels for the case. After preprocessing the sample data, we train the model and perform the task of classifying cases through the learned model. The classification results are given as probability values between 0 and 1 for each LoS, pocket, and bag used to determine the NLoS situation.

There are three categories of typical examples of specific NLoS: (1) Case where the personal device is in a person's hand, (2) Case where the personal device is in the pocket, and (3) Case where the personal device is in the bag. In these three cases, we train deep learning-based classifiers with measured CIR and distance data. The learned classifier calculates the probability of LoS and NLoS when new distance and CIR information are provided as input. The probabilities to NLoS of the measurement are determined by using it to calculate the Kalman gain of the Kalman filter, which corrects the distance data through the calculated probability. This can make the Kalman filter's predictions more accurate by trusting the system's predictions rather than trusting the measured data under unfavorable measurement conditions.

Our system consists of four main components, including the learning stages of deep learning models. The first component uses CIR and distance data to learn classification models based on deep learning. Deep learning models can use stochastic inferences by quantifying ambiguous channel situations by computing probabilities of LoS and NLoS through the application of the softmax function. The data used for learning improves the performance of the classifier by collecting 1016 CIR data from the pocket and the bag for a long time. Training data are collected from about 30,000 pieces of data in each environment. Deep learning models learned in the second component obtain probabilities for LoS, and NLoS when real UWB range data are input and pass this probability information and distance data as input to the third element, Kalman Filter-based distance error correction algorithm. The third component receives LoS and NLoS probability information and distance data and adjusts the error matrix of contextual Q. The Kalman gain is determined based on the determined Q and R. This process can improve the distance error correction performance of the Kalman filter. We calculated the position data using the trilateration
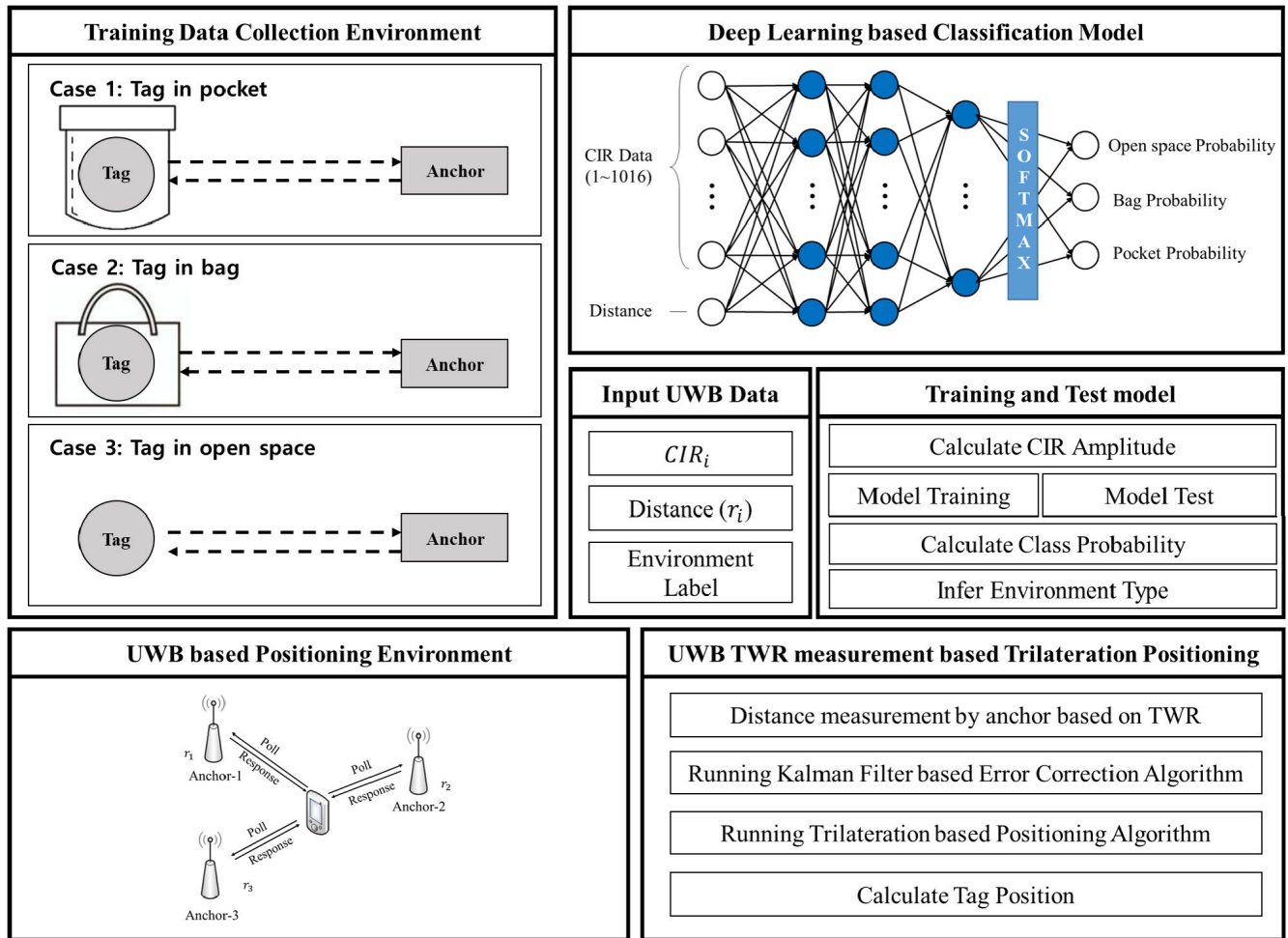
FIGURE 8. Proposed UWB-based positioning system architecture.

positioning algorithm based on the distance data corrected in the fourth element.

The proposed position estimation algorithm improves the accuracy of location estimation by reflecting the probability inference that measurements have for NLoS when calculating Kalman gain for distance data. FIGURE 9 shows the proposed ranging measurement correction algorithm using the deep learning model and weighted adaptive Kalman filter (WAKF). FIGURE 10 depicts the operation of the Kalman filter to calibrate the ranging measurement.

B. PROPOSED DEEP LEARNING MODEL
We use a DNN model as a classification model using deep learning to learn CIR data, which is used as a core in our system. The DNN model can learn the properties of data regardless of continuous or categorical types, and the higher the amount of data when extracting features of data, the higher the prediction accuracy generally compared to other machine learning techniques.

It can also be used for applications that require rapid calculation because it can classify data quickly and accurately.

To use the DNN model, we divided it into learning stages and classification stages. During the learning phase, the learning data is used as 80% and 20% test data of the entire collection data. The data used for learning is the collection of NLoS data from the bag and pocket environment and the LoS data from the open environment. The accuracy of mobile phone distance measurement depends on the distance between the tag and the anchor measurement terminal.

However, due to the nature of the mobile phone, there is a possibility that distance measurement accuracy may be compromised by dynamic movement and various obstacles, so special environmental factors should be considered. For example, there may be an NLoS path even if the distance is close, or there may be an LoS path even if it is further away. Therefore, UWB learning data was acquired according to distance and environment.

The learning data collected 30,000 datasets in each of the two NLoS situations and 30,000 datasets in the LoS situations to obtain specific characteristics of the NLoS situations, consisting of 90,000 total datasets. This is a data acquisition environment assuming the two most likely NLoS situations
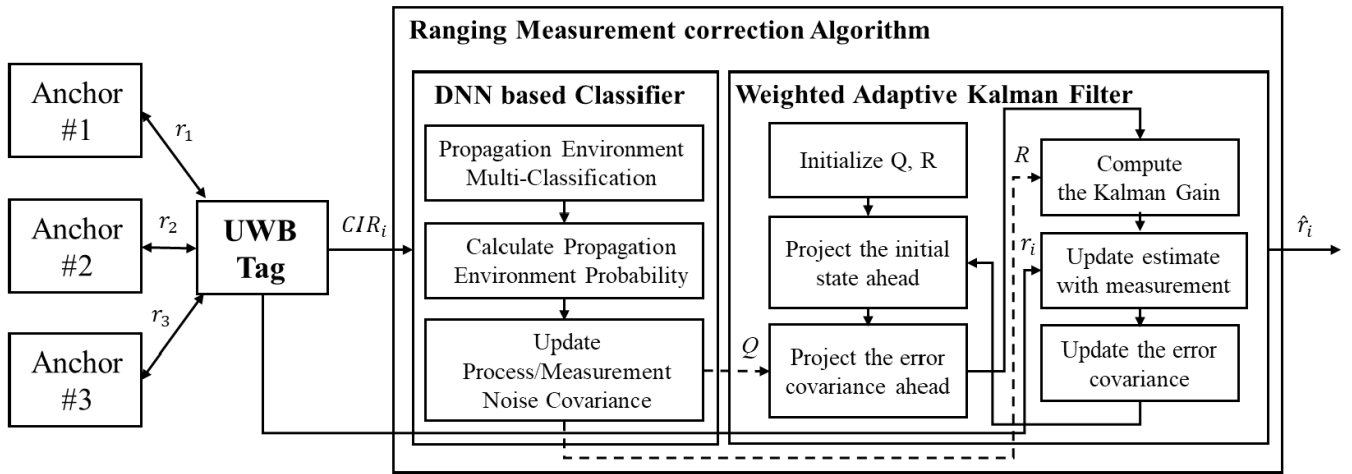
FIGURE 9. Proposed ranging measurement correction algorithm.
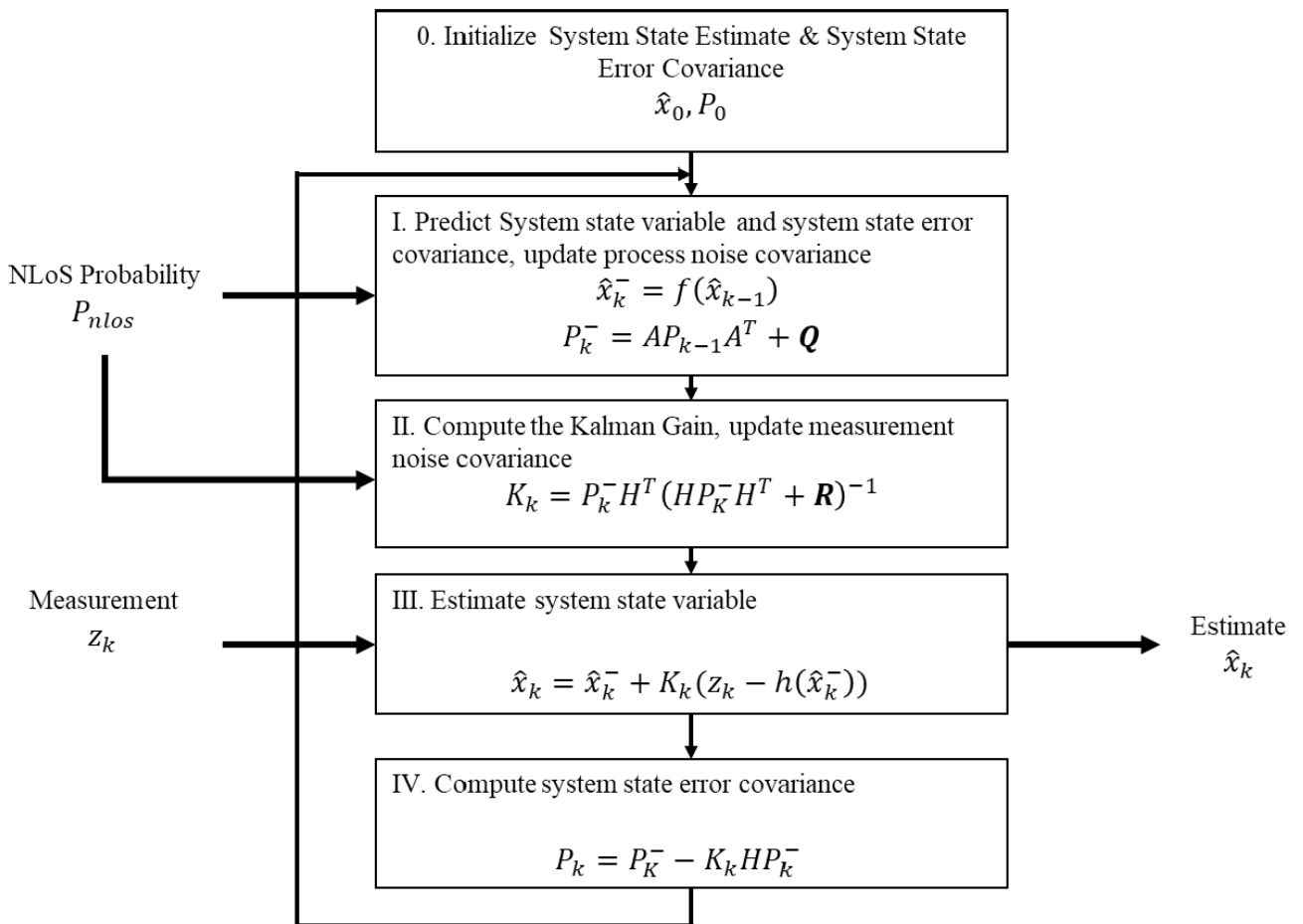

FIGURE 10. Ranging measurement correction process based on Kalman Filter.

so that the location target characteristics of the mobile phone can be well considered. To prevent feature bias in the data, we learned by collecting data sets at a similar rate across all environments. The ratio of the learning data is collected as close to 1:1:1 as possible for a bag, pocket, and open space, but we have trained the model by increasing the proportion of the data that we want in the deep learning model for better classification.

During the classification phase that utilizes the deep learning model, distance and CIR data are extracted from the actual positioning sites, and then the probability for the type of propagation environment is calculated using the DNN classification model. The activation function used in the model used the softmax function, and the probability value for the type of propagation environment is output. The prediction result of the model is defined as a real number between 0 and 1, and the sum of the total output data is 1.

C. PROPOSED KALMAN FILTER-BASED DISTANCE CORRECTION ALGORITHM

The UWB theoretically transmits a pulse signal and must receive a pulse signal, but the received signal arrives reflecting the characteristics of the channel through which the signal is propagated.

The received signal can be used to verify the reliability of the TWR measurement between the UWB anchor and the tag. This measurement reliability is used as a key parameter for the Kalman filter.

The Kalman filter consists largely of prediction and update phases. The prediction step defines a system model and predicts the following states based on the defined system model. The update phase calculates the Kalman gain, weights the predicted state and measurements in the prediction phase, and updates the state estimates. The system model was modeled assuming a constant velocity model.

In the Kalman filter, it is determined by Kalman gain that the system prediction model or measurement model is more reliable in predicting the following conditions. We used a DNN-based classification model to adjust the Kalman gain according to the classified channel type.

This method can compensate for the distance error value of the environment by giving more weight to the system prediction model of the Kalman filter in environments where accurate ranging is difficult.

Initialize Q and R in the behavior of the initial Kalman filter: system noise condition, and measurement noise condition, respectively. It then initializes the predictive value of the system's initial state and the state error covariance.

From the next behavior of the Kalman filter, the system model predicts the next state variable as shown in (8).

$$\hat{x}_t^- = A\hat{x}_{t-1} + Bu_t \qquad (8)$$

The results of the DNN-based classification model determine Q and R to obtain the process noise covariance, as shown in (9), (10).

$$P_t^- = AP_{t-1}A^T + Q \qquad (9)$$
$$K_t = P_t^- H^T (HP_t^- H^T + R)^{-1} \qquad (10)$$

We can construct an error matrix that reflects different error matrices depending on the channel state estimated in real time.

The process noise covariance and R calculate the new Kalman gain, predict the system state variables from the determined Kalman gain and distance measurements, and update the system state error covariance as shown in (11), (12).

$$\hat{x}_t = \hat{x}_t^- + K_t(z_t - \hat{x}_t^-) \qquad (11)$$
$$P_t = (I - K_t H)P_t^- \qquad (12)$$

The predicted value of the system state variable is the output of the Kalman filter and the corrected distance data we are trying to obtain.

The state transition expression for the prediction phase is as follows:

$$x_t = \begin{bmatrix} s(t) \\ v(t) \end{bmatrix} \qquad (13)$$

$$x_t = Ax_{t-1} = \begin{bmatrix} 1 & \Delta t \\ 0 & 1 \end{bmatrix} x_{t-1} \qquad (14)$$

$$z_t = D_t \qquad (15)$$

where D_t is the UWB ranging measurement at time t.

D. PROPOSED TRILATERATION-BASED POSITIONING ALGORITHM

We use the trilateration positioning algorithm to determine the final position through the corrected distance data. Each of the measured distance data from the three anchors is calibrated and used as an input to the final positioning algorithm.

The trilateration-based positioning method is calculated by (16)-(29).

1. Define the equations of three circles

$$(x - x_1)^2 + (y - y_1)^2 = r_1^2 \qquad (16)$$
$$(x - x_2)^2 + (y - y_2)^2 = r_2^2 \qquad (17)$$
$$(x - x_3)^2 + (y - y_3)^2 = r_3^2 \qquad (18)$$

2. l_1 Equation of a straight line passing through the intersection of circles 1 and 2

$$2(x_2 - x_1)x + 2(y_2 - y_1) = r_1^2 - r_2^2 - x_1^2 + x_2^2 - y_1^2 + y_2^2 \qquad (19)$$
$$2(x_3 - x_2)x + 2(y_3 - y_2) = r_2^2 - r_3^2 - x_2^2 + x_3^2 - y_2^2 + y_3^2 \qquad (20)$$

3. Expression for x, y

$$A = 2(x_2 - x_1) \qquad (21)$$
$$B = 2(y_2 - y_1) \qquad (22)$$
$$C = r_1^2 - r_2^2 - x_1^2 + x_2^2 - y_1^2 + y_2^2 \qquad (23)$$
$$D = 2(x_3 - x_2) \qquad (24)$$
$$E = 2(y_3 - y_2) \qquad (25)$$
$$F = r_2^2 - r_3^2 - x_2^2 + x_3^2 - y_2^2 + y_3^2 \qquad (26)$$
$$Ax + By = C \qquad (27)$$
$$Dx + Ey = F \qquad (28)$$
$$\begin{bmatrix} x \\ y \end{bmatrix} = \begin{bmatrix} A & B \\ D & E \end{bmatrix}^{-1} \begin{bmatrix} C \\ F \end{bmatrix} \qquad (29)$$

IV. EVALUATION

This section describes the assessment of the proposed accurate positioning system. This section is described in the following order: Description of experimental environment and equipment installation, setup of data sets for experiments, performance evaluation of classification models based on deep learning, evaluation of position from proposed distance correction algorithm, comparing experimental results with position from existing Kalman filter-based correction algorithm and calculated position.

A. EXPERIMENTAL SETUP

1) SETUP FOR ENVIRONMENTS

The experiment was conducted in the lobby of the Fusion Tech Center building at Hanyang University's Seoul Campus in South Korea. To experiment with UWB-based accurate positioning algorithms, we use the SS-TWR method as UWB ranging method. The UWB device used in the experiment is Qorvo's DWM3000.

The DWM3000 equipment weighs 200g and is 7cm wide and 13.3cm long, similar to a regular mobile phone. The applied UWB chipset is the DW3000 in Qorvo. The DW3000 is a fully integrated single chipset and complies with the IEEE 802.15.4z [39] standard. UWB Communication Channel 5 (6.5 GHz) was used.

For the positioning experiments, we used three anchors to cover a rectangular positioning area measuring 11 m wide and 11 m long. In the experiment, the DWM3000 acts as both an anchor and a tag and consists of three anchors and one tag.

Each anchor station consists of three fixed anchor stations, each serving as a responder for TWR communications. In the experiment, the tags communicate with the anchors to transmit the measured CIR and distance data to the server running the deep learning model and positioning engine.

Each anchor is installed in a fixed position 2.5 meters high relative to the antenna module, with anchor 1 at (0,0) (meters), anchor 2 at (11,0) (meters), and anchor 3 at (11,11) (meters). Installing each anchor station at a constant height increases the accuracy of the positioning results.

For accurate CIR measurements, the module is installed with the orientation facing the inside of the positioning area. Our positioning experiment is a square measuring 8.5 meters by 9.5 meters, and the transceiver antenna is installed at 45 degrees toward the center of the square. Antenna angles for each anchor station are configured arbitrarily and may contain errors. Fine setting of antenna angles is not an essential factor to consider because this work aims to improve the accuracy of Kalman filter position estimation according to CIR analysis.

To establish a reference path for positioning, a person moved into a rectangular positioning area consisting of an anchor station with a mobile phone in three ways: inside a bag, inside a pocket, and in an open space estimated into a hand. FIGURES 11 and 12 show the UWB DWM3000 equipment and installation environment used in the experimental evaluation.

FIGURE 11. DWM3000 and NUCLEO F429ZI Development kit.

We selected three LoS, NLoS scenarios as an experiment in which the proposed deep learning-based classification model improves the positioning accuracy by reducing the ranging error occurring in the NLoS situation of the personal device: The scenario of moving with the tag on hand, the scenario of moving the tag in the bag, the scenario of moving the tag in the pocket. Three experimental scenarios for evaluating the proposed algorithmic settings are shown in FIGURES 13, 14, and 15.

2) SETUP FOR DATASETS

The dataset used in the experiment is the amplitude data of the CIR measured at the same time as the distance measurement. Distance measurements include errors due to design errors in the equipment itself, the location of objects present in the indoor environment, and the material of the objects.

To obtain more accurate location data, a process of correcting the errors contained in this distance measurement is required. The CIR data is an indicator of the quality of the UWB communication channel and can be used to compensate for errors in distance measurements.

Our CIR data acquisition environment is an environment in which tag and anchor act as initiators and responders, respectively, and communicate through SS-TWR. Here, TWR was performed between the anchor and the tag with LoS path, as well as between the anchor and the tags in the pocket and the bag. In addition, we also extracted CIR through the ranging measurement.

We have divided the NLoS path into two cases to allow deep learning models to learn specific features about the NLoS path through multi-classification. Finally, We obtained CIR data assuming three scenarios. The three scenarios include the open space, the pocket, and the bag. And the distances between the tag and the anchor are 8, 9, and 10 meters, respectively. The proportions of CIR data collected for distances of 8, 9, and 10 m for tags in the bag, the pocket, and the open space are shown in FIGURE 16 and are used as learning data for deep learning.

FIGURE 12. Installation of UWB anchors in experimental environment.

FIGURE 14. Indoor positioning experimental environment for tags in pocket.

FIGURE 15. Indoor positioning experimental environment for tags in bag.
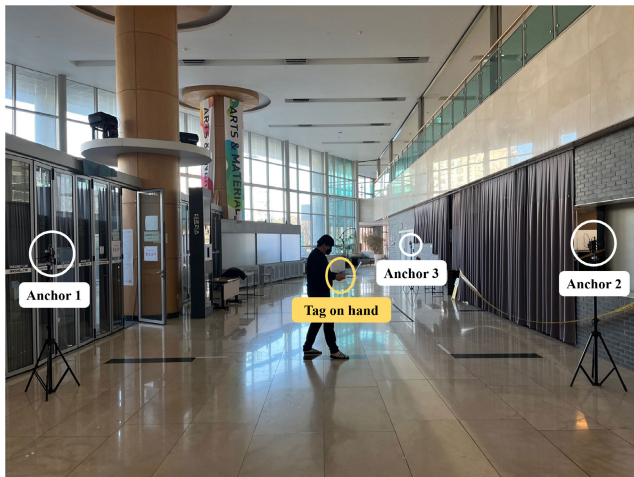

FIGURE 13. Indoor positioning experimental environment for tags on hand.

The total number of learning data is 90,000, and each of the three wireless environments consists of 30,000 data. Deep learning-based propagation environment multi-classifiers use this CIR data to classify open space, bag, and pocket. We had 1,016 CIR data in one TWR we acquired, but the data meaningful for interpretation was after the first path, so we extracted CIR data from 850ns and later. Each plot shows the amplitude distribution of the CIR over the time axis for all samples from which the learning data was obtained.

FIGURE 17 shows a top view of the amplitude distribution of real numbers and imaginary numbers in the CIR data in three propagation environments between the UWB transmitter and the UWB receiver. Since the actual positioning environment is a typical indoor environment rather than a chamber, there are many indirect path signals due to the surrounding walls and multipath. To enable deep learning models to learn this better, the learning data acquisition environment has acquired CIR data in a more realistic environment as a laboratory environment, not an anechoic chamber. For example, the CIR amplitude near index 7500 is indented compared to other indexes, as shown in FIGURE 17 (b), which can be seen as a signal degradation caused by multipath present in the environment.

FIGURE 17 (a)-(c) shows the amplitude of the CIR that appears when it is 8, 9, and 10 m away from the anchor fixed to the tag in the open space. In FIGURE 17 (a), we can see that the peak is maintained without noise, but in FIGURE 17 (b), we can see that noise is included due to multipath from the surrounding environment as the distance increases. Since these noises are so small that they can occur when the tag moves, we used the corresponding data containing noise in the learning as it is to enable the deep learning model to learn efficiently.
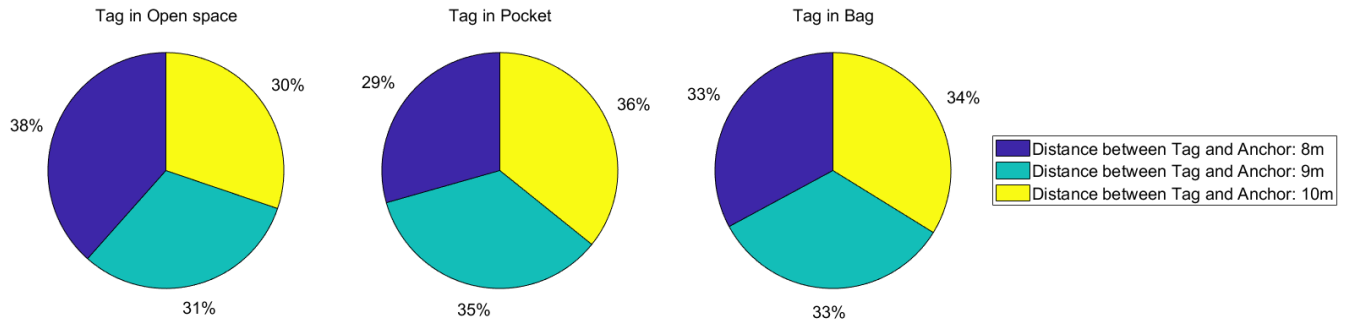
FIGURE 16. Ratio of CIR data obtained in three scenarios.
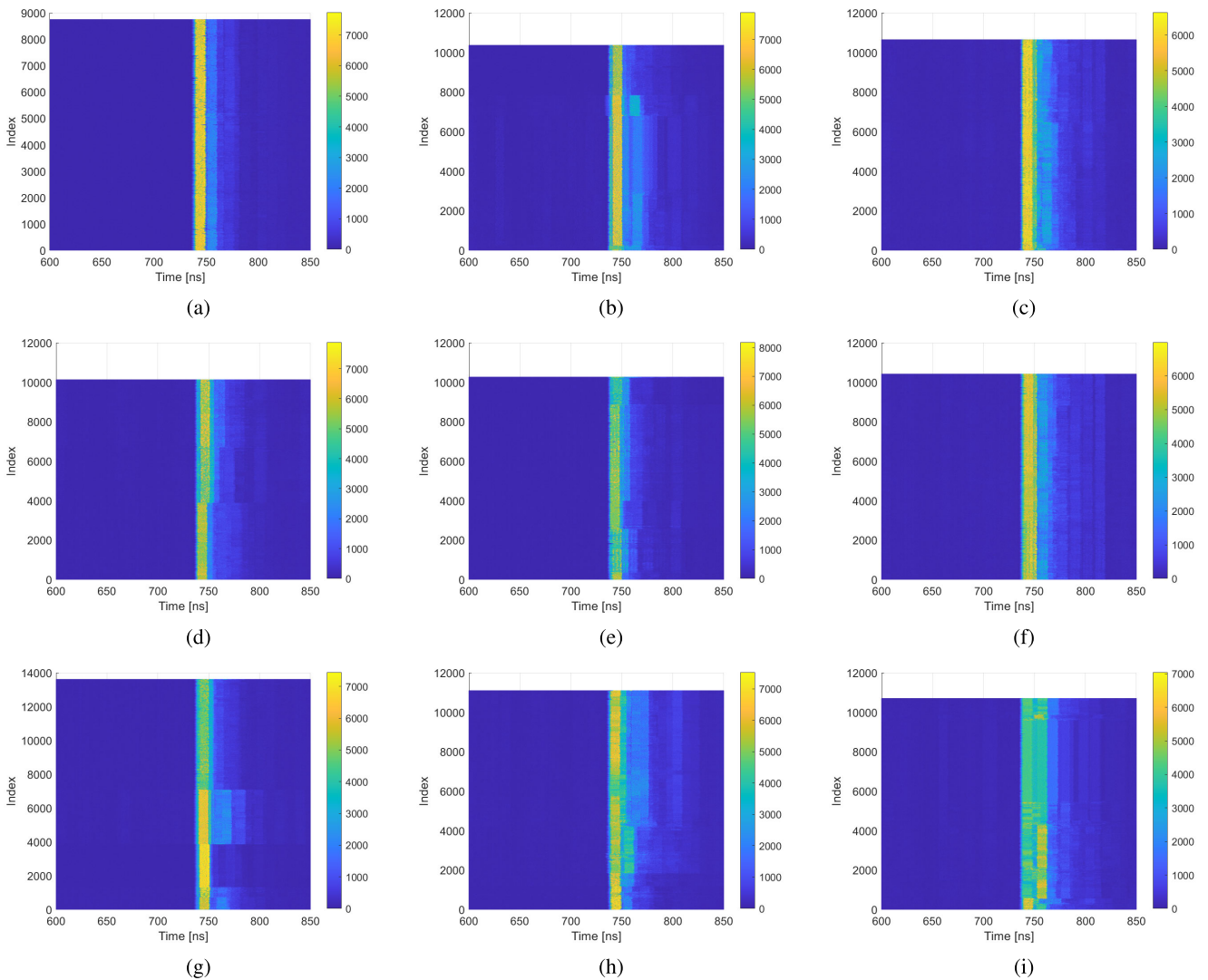

FIGURE 17. The top view of the learning data (CIR amplitude) distribution: (a)-(c) CIR amplitude measured at the tag in open space 8 m (a), 9 m (b), 10 m (c) away from the anchor, respectively; (d)-(f) CIR amplitude measured at the tag in pocket 8 m (a), 9 m (b), 10 m (c) away from the anchor, respectively; (g)-(i) CIR amplitude measured at the tag in bag 8 m (a), 9 m (b), 10 m (c) away from the anchor, respectively.

FIGURE 17 (d)-(f) shows the amplitude of the CIR that appears when it is 8, 9, and 10 m away from the anchor fixed to the tag in the pocket. Compared to other distances, we can see that the peak of the CIR decreases as the distance between the tag and the anchor increases. The propagation path between the anchor and the tag in FIGURE 17 (e) is

NLoS, and the amplitude of the CIR is unevenly distributed as the distance increases, as there is an obstruction to the signal from the tag in the pocket. We can see that the maximum amplitude of the CIR has also decreased as moves to 10 m.

FIGURE 17 (g)-(i) shows the CIR amplitude at 8, 9, and 10 m from the anchor in the bag in the fixed anchor and NLoS path. Like tags in pockets, there is no LoS path between anchors, so the amplitude of the CIR is unevenly distributed as the distance increases, but the signal is more disturbed by items in the bag, such as books and laptops, compared to tags in the pocket. Moving to 10 m, we can see that the maximum amplitude of the CIR is difficult to distinguish signals by multipath.

Compared with FIGURE 17 (f) and (i), we can see that the CIR magnitude peak in FIGURE 17 (c) is constant and produces less noise. In addition, the maximum amplitude of the CIR measured at the same distance by the environment was most pronounced in the open space.

B. DNN-BASED CLASSIFICATION RESULTS

To improve the positioning accuracy of the position error correction algorithm, we trained a DNN-based deep learning classification model using distance-specific CIR learning data. The proposed deep learning model learns from a preprocessed dataset by assigning labels corresponding to propagation environments where tags were placed during a single TWR, simultaneously with 1016 amplitude data from CIR measured as learning data from deep learning models.

Depending on the characteristics of the mobile phone, the learning data are constructed by specifying the situation in which the mobile phone may exist with high probability in the pocket and bag so that the contextual CIR characteristics can be learned better by the deep learning model. Deep learning models can learn the propagation environment according to CIR amplitude distribution and distance.

Experiments in the position error correction algorithm perform SS-TWR between the UWB tag and the anchor and use the obtained CIR and distance data as inputs to the pre-trained deep learning model. The deep learning model uses the acquired data to classify which class the propagation environment of the current tag belongs to and outputs it as probability data. The softmax-based activation function then obtains the sum of all class probabilities as 1 with a probability between 0 and 1 by weighing the Kalman filter's measurement model and the system prediction model using the output from the deep learning model.

FIGURES 18 and 19 show graphs for classification accuracy and loss of deep learning models, respectively. In FIGURE 18, the model accuracy reached stable 0.99 after 40 epochs. Also, FIGURE 19 shows the model loss appears to be less than 0.1 after 40 epochs. We see that the proposed model achieves a higher classification of accuracy as the epoch of learning continues.

C. POSITIONING RESULTS

This section tests the proposed positioning system for indoor UWB personal devices. To verify the correction level, the
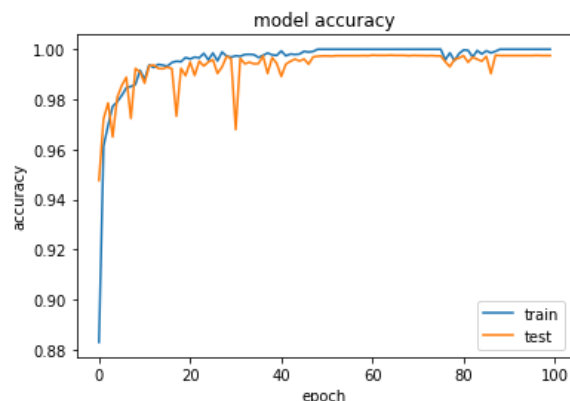

FIGURE 18. Training and test accuracy of proposed DNN model.
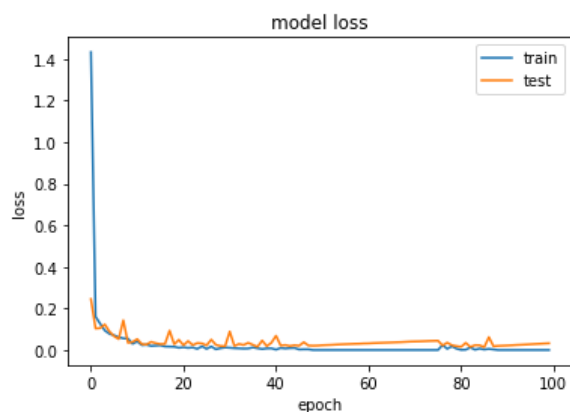

FIGURE 19. Training and test loss of proposed DNN model.

proposed trilateration-based positioning algorithm compares the trilateration positioning calculated from UWB-based TWR measurement data with the positioning result calculated from ranging data corrected using the KF estimator and the positioning result of our proposed WAKF.

In our experiments, we possess UWB in two representative ways since we cannot obtain accurate knowledge of the various environmental-specific UWB TWR measurement errors of mobile phones in multiple positions. The situation of having a mobile phone is divided into the case of putting a mobile phone in a bag, putting it in a pocket, and carrying it in hand, just like how learned learning data.

Positioning is performed using TWR-based trilateration positioning with 5 position calculations per second.

It is judged that it is difficult to trust the measured value if the output value classified by the tag of the pocket and bag is close to 1, so increase the value of the process noise covariance and reduce the value of the measured noise covariance of the measured noise. When the noise matrix is set, the Kalman filter adjusts the Kalman gain for the data in that input to output a calibrated distance prediction.

We compared location data calculated from TWR distance data obtained from human travel paths to trilateration-based locations, Kalman Filter-based locations to Kalman Filter-based locations, and WAKF, calculated from distance data
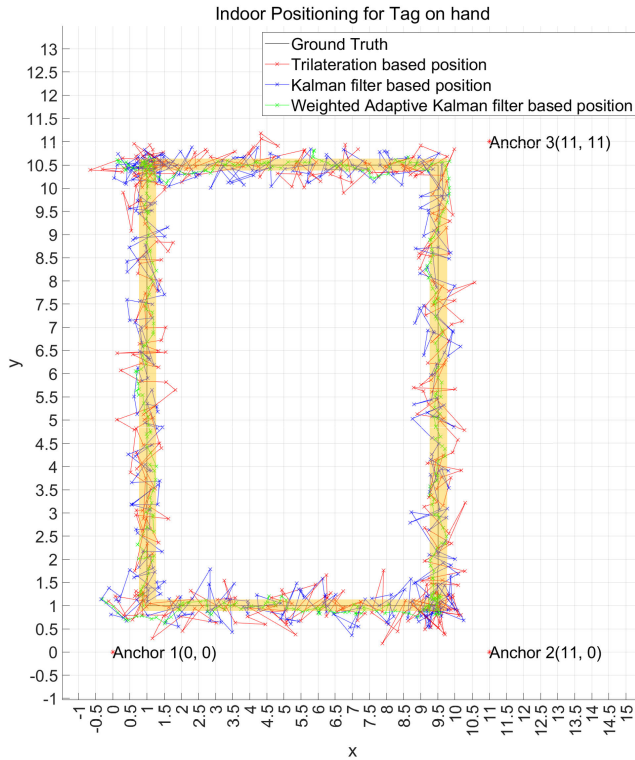
FIGURE 20. Estimated positions of the tag on hand. Red dots are positioned by the trilateration algorithm, blue points are positioned by the normal Kalman filter, and green dots are positioned by the proposed WAKF. The orange area is an area extending by ±50 cm in width based on ground truth.

FIGURE 21. Estimated positions of the tag in the pocket. Red dots are positioned by the trilateration algorithm, blue dots are positioned by the normal Kalman filter, and green dots are positioned by the proposed WAKF. The orange area is an area extending by ±50 cm in width based on ground truth.

corrected by the proposed deep learning-based distance error correction algorithm.

The comparison method thickens the path with a constant ratio of error for ground truth, which is determined to be 8.5 meters × 9.5 meters in size, and compares how much location data is contained inside.

FIGURE 20 shows the results of an experiment in which the UWB terminal moved along a specified path with the UWB terminal on hand. The red dots represent where the distance measurement data were calculated by the trilateration positioning algorithm. The blue dots represent the positions where the trilateration positioning algorithm is calculated from distance data calibrated with a typical Kalman filter. The green dots mark where the trilateration positioning algorithm is calculated from distance data applied with the proposed correction algorithm. We can see the estimated results of applying our proposed algorithm close to the ground truth in black. This shows the distance error occurring in the NLoS situation was accurately classified and estimated.

The orange area in FIGURE 20 has an error tolerance of ±50 cm for ground truth. Within this area, 347 WAKF-based location data, 315 KF-based location data, and 319 general trilateration-based location data were observed. We can see that the proposed algorithm estimated its location more accurately than other algorithms.
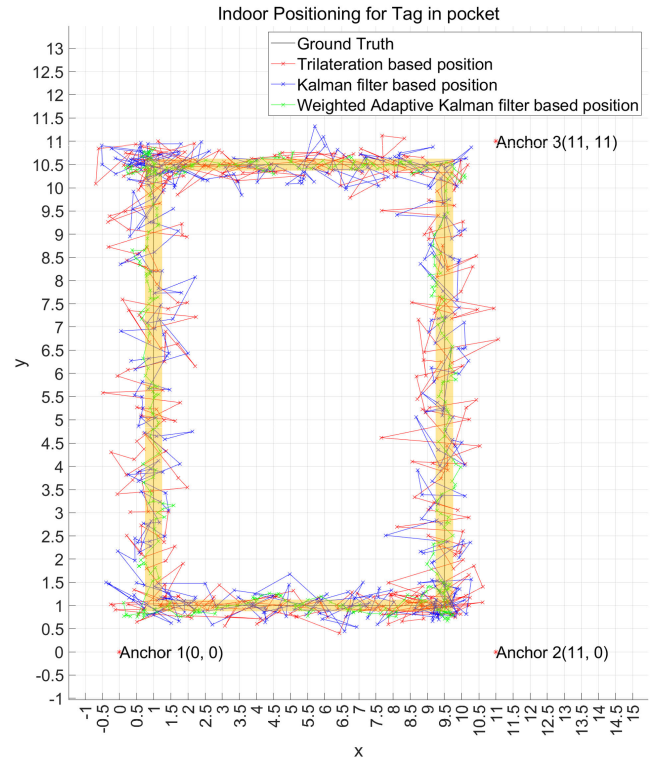
FIGURE 21 shows experimental results when the UWB terminal moved with the UWB terminal in its pocket. The location data based on trilateration shows that the value is more unstable than when moved on hand. We can see the TWR-based distance measurement data contained more errors from NLoS and Multipath. As illustrated in FIGURE 21, the location estimated by our proposed algorithm was closer to the black ground truth; 344 WAKF-based location data, 292 KF-based location data, and 262 trilateration-based location data were observed in the orange area.

FIGURE 22 shows the results of an experiment in which the UWB terminal moved with the UWB terminal in the bag. We can see that the error in the location data is greater compared to the experiments of the hands and pockets. This is because interference factors such as laptops and books in bags that contain terminals have a greater impact on UWB signal propagation, resulting in ranging errors. In the orange area, 342 WAKF-based location data, 262 KF-based location data, and 262 trilateration-based location data were included. The experimental results with ±25 cm and ±100 cm, including ±50 cm, are shown in TABLE 2.

According to TABLE 2, the proposed positioning system improved positioning accuracy by up to 27.22% and at least 20.84% in the ±25 cm of error tolerance, by up to 22.78% and at least 7.78% in the ±50 cm of error tolerance, by up to
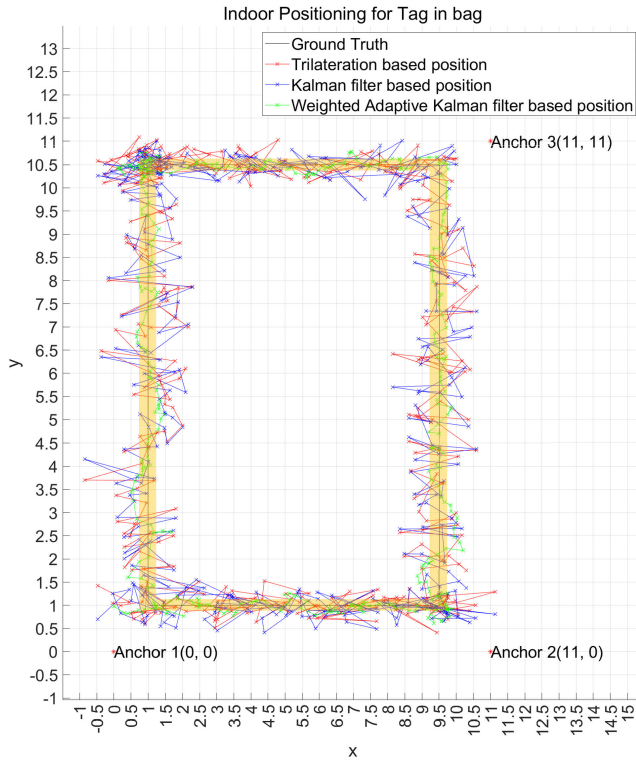
FIGURE 22. Estimated positions of the tag in the bag. Red dots are positioned by the trilateration algorithm, blue dots are positioned by the normal Kalman filter, and green dots are positioned by the proposed WAKF. The orange area is an area extending by ±50 cm in width based on ground truth.

TABLE 2. Accuracy comparison between the proposed approach (WAKF) and traditional approaches (Kalman Filter and Trilateration) for three scenarios with different error tolerances. (Raw data are available upon request*.)

Scenario	Error Tolerance	WAKF (Proposed)	Kalman Filter	Trilateration
Hand	±25cm	90.83%	68.61%	67.78%
	±50cm	96.39%	87.50%	88.61%
	±100cm	99.44%	99.17%	98.89%
Pocket	±25cm	82.78%	61.94%	55.56%
	±50cm	95.56%	81.11%	72.78%
	±100cm	100%	96.39%	91.67%
Bag	±25cm	80.56%	56.67%	56.67%
	±50cm	95.00%	72.78%	72.78%
	±100cm	99.72%	93.33%	93.33%

*Please contact smsung@hanyang.ac.kr for raw data.

8.33% and at least 0.27% in the ±100 cm of error tolerance. A notable result is that the proposed method has nearly 100% accuracy for ±100 cm of error tolerance to the ground truth.

V. CONCLUSION
In this study, we applied UWB technology to provide accurate indoor positioning of personal devices such as mobile phones. Since TWR measurement errors occur in NLoS conditions
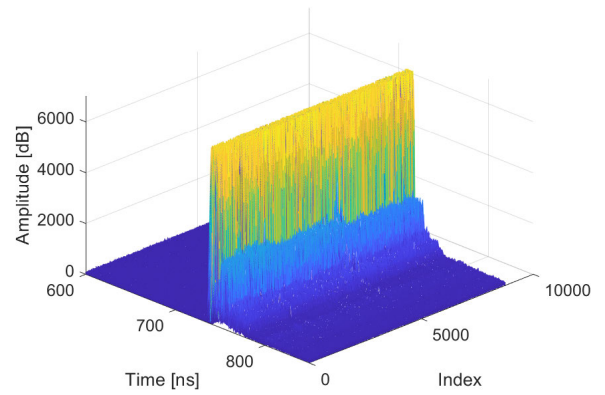

FIGURE 23. Amplitudes of CIR measured at the tag in open space and the anchor at a distance of 8 m.
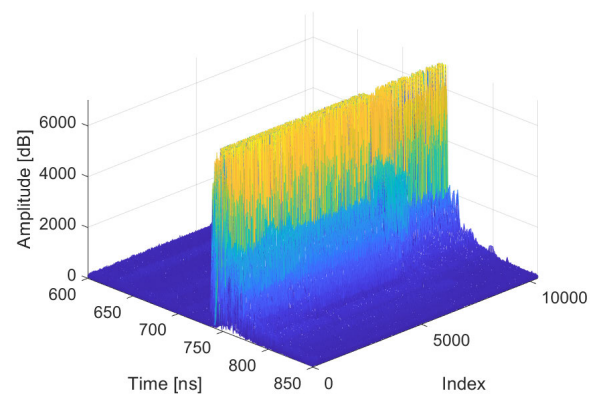

FIGURE 24. Amplitudes of CIR measured at the tag in open space and the anchor at a distance of 9 m.
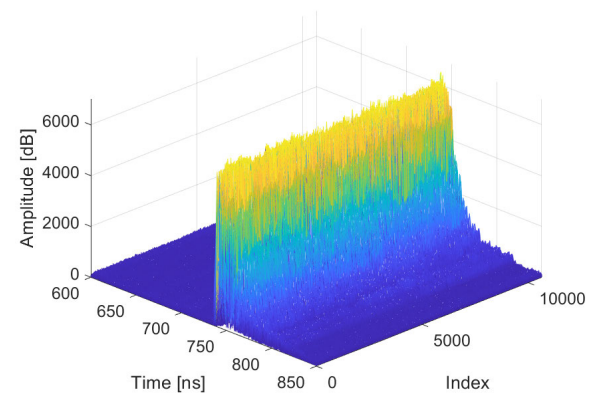

FIGURE 25. Amplitudes of CIR measured at the tag in open space and the anchor at a distance of 10 m.

between UWB terminals, we applied a deep learning-based propagation environment classification model to classify NLoS conditions through UWB CIR and device-to-device distances and perform error correction through the Kalman filter.

At this time, to improve the classification accuracy of the deep learning model, the NLoS conditions were subdivided into consideration of the representative portable method of the mobile phone to collect the learning data.
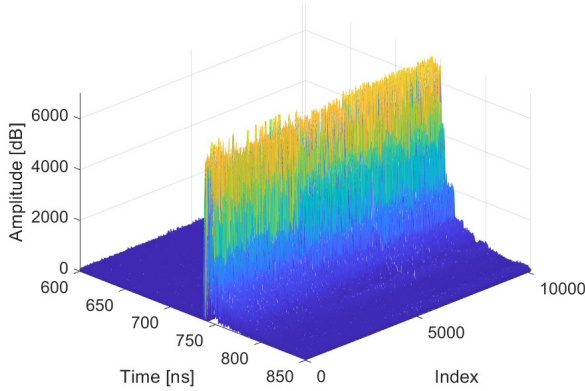
FIGURE 26. Amplitudes of CIR measured at the tag in the pocket and the anchor at a distance of 8 m.
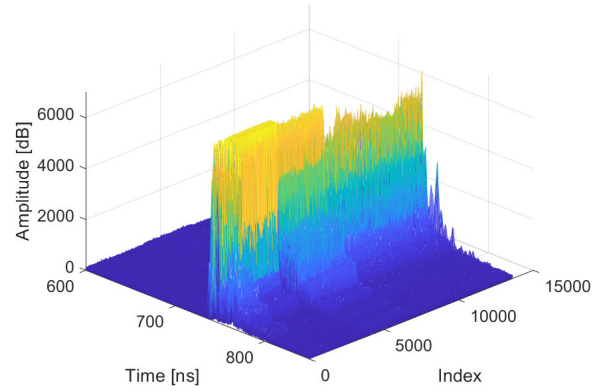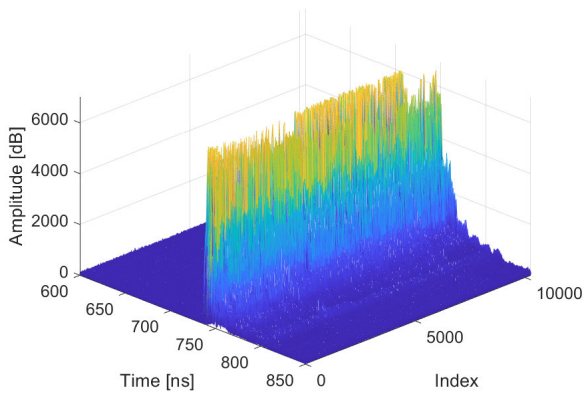

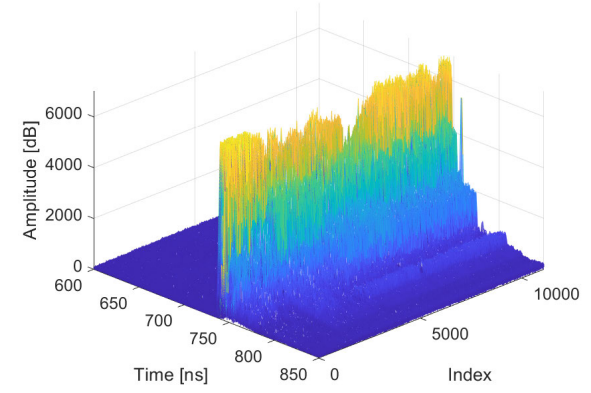**FIGURE 27.** Amplitudes of CIR measured at the tag in the pocket and the anchor at a distance of 9 m.

FIGURE 28. Amplitudes of CIR measured at the tag in the pocket and the anchor at a distance of 10 m.

FIGURE 29. Amplitudes of CIR measured at the tag in the bag and the anchor at a distance of 8 m.

FIGURE 30. Amplitudes of CIR measured at the tag in the bag and the anchor at a distance of 9 m.

FIGURE 31. Amplitudes of CIR measured at the tag in the bag and the anchor at a distance of 10 m.
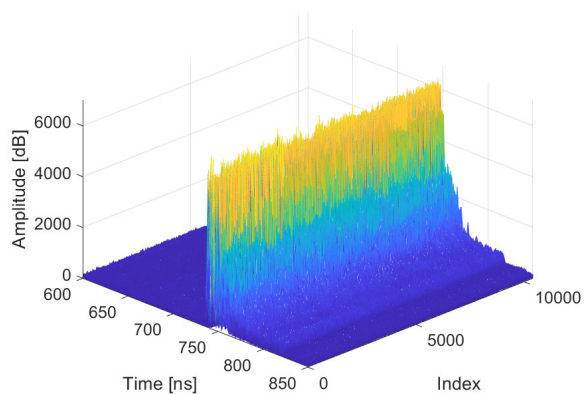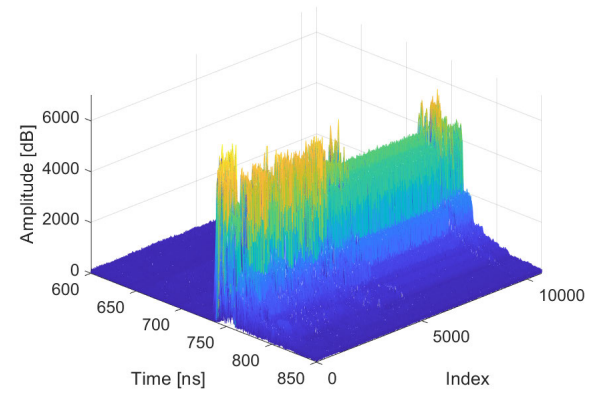
As a result, we developed an indoor precision localization scheme for UWB trilateration-based mobile phones. To reduce the environmental TWR measurement error, WAKF was used as the main estimator, and Kalman gain was adjusted by applying the propagation environment classification results. Experimental results show that the WAKF estimator has been able to significantly reduce errors occurring in typical mobile phone-carrying situations.

Overall, our proposed WAKF-based algorithms for personal devices localization enhances positional accuracy by up to 27.22% with ±25 cm of error tolerance over an unfiltered positioning algorithm and by up to 23.89% with ±25 cm of error tolerance over a typical Kalman filter-based positioning algorithm.

Our approach can be applied to environments where learning data for deep learning has been acquired, and in new and expanded environments, additional learning data and deep
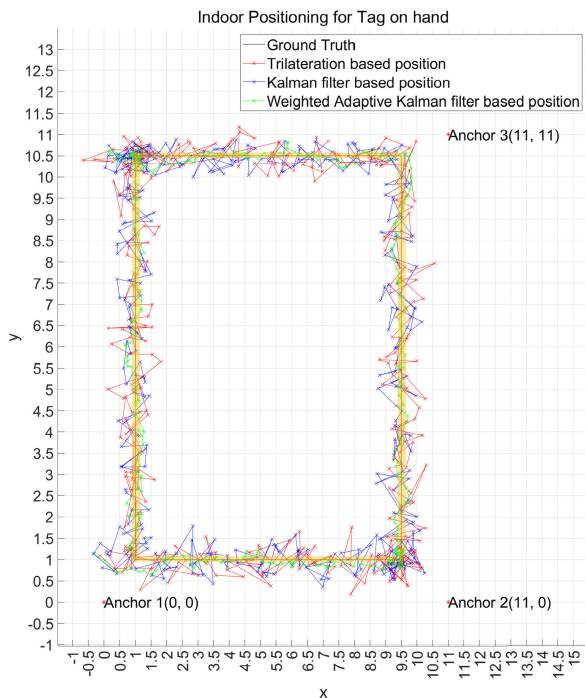
FIGURE 32. Estimated positions of the tag on hand. The orange cover area is an area extending by ±25 cm in width based on ground truth.
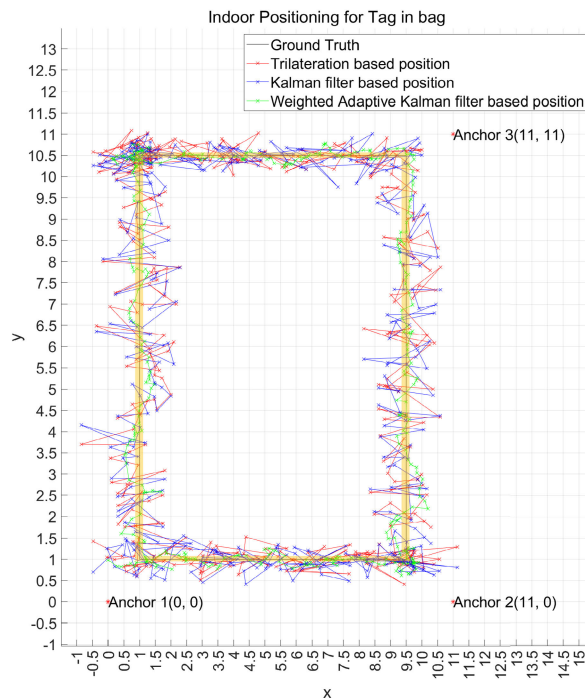

FIGURE 34. Estimated positions of the tag in a bag. The orange cover area is an area extending by ±25 cm in width based on ground truth.

FIGURE 33. Estimated positions of the tag in a pocket. The orange cover area is an area extending by ±25 cm in width based on ground truth.

FIGURE 35. Estimated positions of the tag on hand. The orange cover area is an area extending by ±100 cm in width based on ground truth.

learning models need to be improved. In future research, we will study adaptive deep learning models according to changes in the positioning environment, data learning that does not require improvement of deep learning models, and feedback learning methods that can automatically calculate system errors/measurement errors of the Kalman filter.

APPENDIX

FIGURES 23-31 illustrate amplitudes of CIR measured under different environments (an open space, a pocket, and a bag) at different distances (8 m, 9 m, and 10 m).

FIGURES 32-37 demonstrate estimated positions of the tag under different environments (a hand, a pocket, and
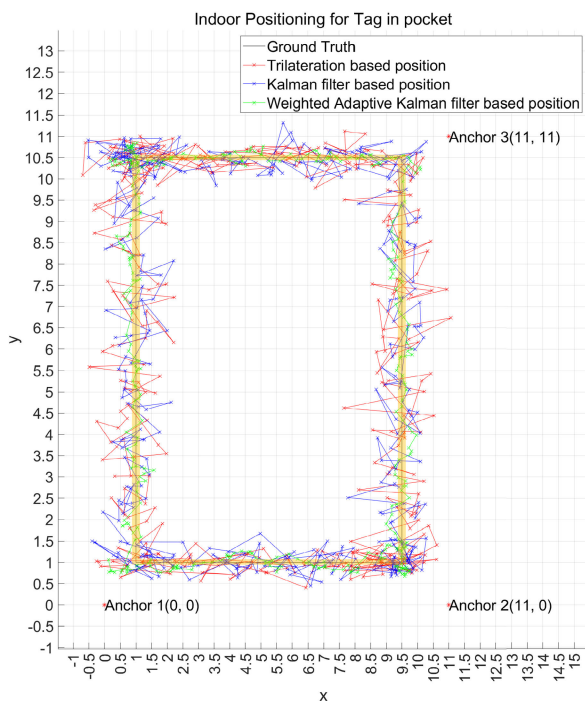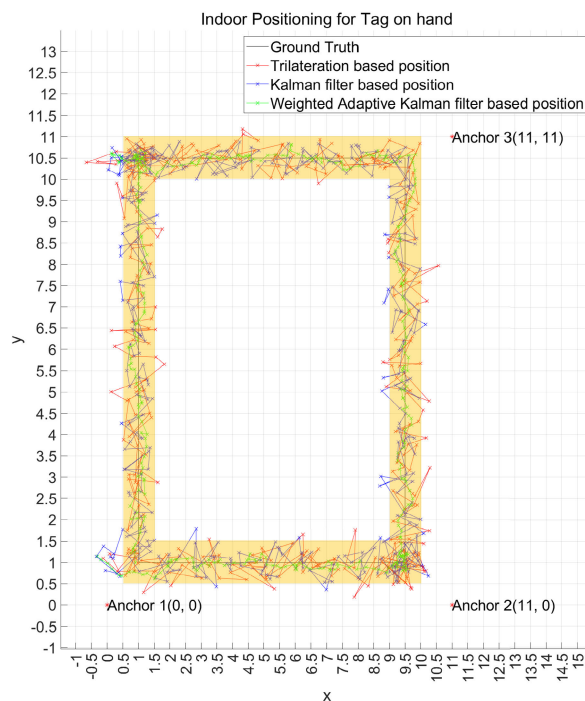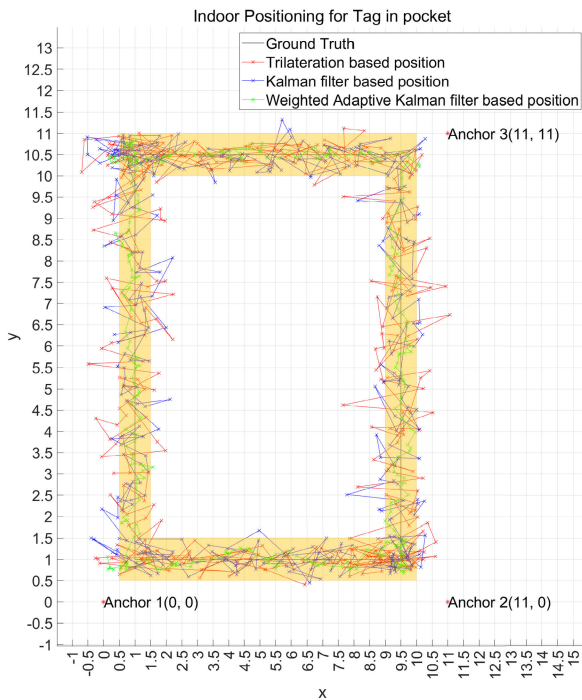
FIGURE 36. Estimated positions of the tag in a pocket. The orange cover area is an area extending by ±100 cm in width based on ground truth.
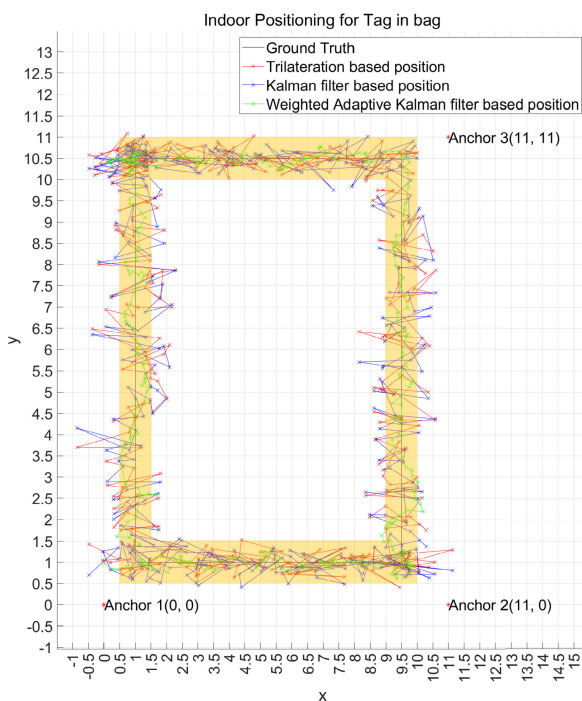

FIGURE 37. Estimated positions of the tag in a bag. The orange cover area is an area extending by ±100 cm in width based on ground truth.

a bag) and different error tolerances (from ± 25 cm to ± 100 cm).

REFERENCES

[1] Y. Cai, W. Guan, Y. Wu, C. Xie, Y. Chen, and L. Fang, "Indoor high precision three-dimensional positioning system based on visible light communication using particle swarm optimization," *IEEE Photon. J.*, vol. 9, no. 6, pp. 1–20, Dec. 2017.

[2] C. Yang and H.-R. Shao, "WiFi-based indoor positioning," *IEEE Commun. Mag.*, vol. 53, no. 3, pp. 150–157, Mar. 2015.

[3] Y. Tao and L. Zhao, "A novel system for WiFi radio map automatic adaptation and indoor positioning," *IEEE Trans. Veh. Technol.*, vol. 67, no. 11, pp. 10683–10692, Nov. 2018.

[4] L. Bai, F. Ciravegna, R. Bond, and M. Mulvenna, "A low cost indoor positioning system using Bluetooth low energy," *IEEE Access*, vol. 8, pp. 136858–136871, 2020.

[5] T.-M.-T. Dinh, N.-S. Duong, and K. Sandrasegaran, "Smartphone-based indoor positioning using BLE iBeacon and reliable lightweight fingerprint map," *IEEE Sensors J.*, vol. 20, no. 17, pp. 10283–10294, Sep. 2020.

[6] J. Larranaga, L. Muguira, J.-M. Lopez-Garde, and J.-I. Vazquez, "An environment adaptive ZigBee-based indoor positioning algorithm," in *Proc. Int. Conf. Indoor Positioning Indoor Navigat.*, Sep. 2010, pp. 1–8.

[7] Y. You and C. Wu, "Hybrid indoor positioning system for pedestrians with swinging arms based on smartphone IMU and RSSI of BLE," *IEEE Trans. Instrum. Meas.*, vol. 70, pp. 1–15, 2021.

[8] Y. Xu, Y. S. Shmaliy, Y. Li, X. Chen, and H. Guo, "Indoor INS/LiDAR-based robot localization with improved robustness using cascaded FIR filter," *IEEE Access*, vol. 7, pp. 34189–34197, 2019.

[9] Q. Zou, Q. Sun, L. Chen, B. Nie, and Q. Li, "A comparative analysis of LiDAR SLAM-based indoor navigation for autonomous vehicles," *IEEE Trans. Intell. Transp. Syst.*, vol. 23, no. 7, pp. 6907–6921, Jul. 2022.

[10] H. Liu, H. Darabi, P. Banerjee, and J. Liu, "Survey of wireless indoor positioning techniques and systems," *IEEE Trans. Syst., Man, Cybern. C, Appl. Rev.*, vol. 37, no. 6, pp. 1067–1080, Nov. 2007.

[11] J. Wisanmongkol, L. Klinkusoom, T. Sanpechuda, L.-O. Kovavisaruch, and K. Kaemarungsi, "Multipath mitigation for RSSI-based Bluetooth low energy localization," in *Proc. 19th Int. Symp. Commun. Inf. Technol. (ISCIT)*, Sep. 2019, pp. 47–51.

[12] W. Xue, W. Qiu, X. Hua, and K. Yu, "Improved Wi-Fi RSSI measurement for indoor localization," *IEEE Sensors J.*, vol. 17, no. 7, pp. 2224–2230, Apr. 2017.

[13] J. Neburka, Z. Tlamsa, V. Benes, L. Polak, O. Kaller, L. Bolecek, J. Sebesta, and T. Kratochvil, "Study of the performance of RSSI based Bluetooth smart indoor positioning," in *Proc. 26th Int. Conf. Radioelektronika (RADIOELEKTRONIKA)*, Apr. 2016, pp. 121–125.

[14] C. C. Pu and W. Y. Chung, "Mitigation of multipath fading effects to improve indoor RSSI performance," *IEEE Sensors J.*, vol. 8, no. 11, pp. 1884–1886, Nov. 2008.

[15] R. D. Ainul, S. Wibowo, and M. Siswanto, "An improved indoor RSSI based positioning system using Kalman filter and MultiQuad algorithm," in *Proc. Int. Electron. Symp. (IES)*, Sep. 2021, pp. 558–564.

[16] F. Zafari, A. Gkelias, and K. K. Leung, "A survey of indoor localization systems and technologies," *IEEE Commun. Surveys Tuts.*, vol. 21, no. 3, pp. 2568–2599, 3rd Quart., 2017.

[17] D. Coppens, A. Shahid, S. Lemey, B. Van Herbruggen, C. Marshall, and E. De Poorter, "An overview of UWB standards and organizations (IEEE 802.15.4, FiRa, Apple): Interoperability aspects and future research directions," *IEEE Access*, vol. 10, pp. 70219–70241, 2022.

[18] Y. Cheng and T. Zhou, "UWB indoor positioning algorithm based on TDOA technology," in *Proc. 10th Int. Conf. Inf. Technol. Med. Educ. (ITME)*, Aug. 2019, pp. 777–782.

[19] S. Bottigliero, D. Milanesio, M. Saccani, and R. Maggiora, "A low-cost indoor real-time locating system based on TDOA estimation of UWB pulse sequences," *IEEE Trans. Instrum. Meas.*, vol. 70, pp. 1–11, 2021.

[20] I. Guvenc, C.-C. Chong, and F. Watanabe, "NLOS identification and mitigation for UWB localization systems," in *Proc. IEEE Wireless Commun. Netw. Conf.*, 2007, pp. 1571–1576.

[21] Q. Tian, K. I. Wang, and Z. Salcic, "Human body shadowing effect on UWB-based ranging system for pedestrian tracking," *IEEE Trans. Instrum. Meas.*, vol. 68, no. 10, pp. 4028–4037, Oct. 2019.

[22] B. Denis, J. Keigmart, and N. Daniele, "Impact of NLOS propagation upon ranging precision in UWB systems," in *Proc. IEEE Conf. Ultra Wideband Syst. Technol.*, Nov. 2003, pp. 379–383.

[23] B. Silva and G. P. Hancke, "Ranging error mitigation for through-the-wall non-line-of-sight conditions," *IEEE Trans. Ind. Informat.*, vol. 16, no. 11, pp. 6903–6911, Nov. 2020.

[24] S. K. Meghani, M. Asif, F. Awin, and K. Tepe, "Empirical based ranging error mitigation in IR-UWB: A fuzzy approach," *IEEE Access*, vol. 7, pp. 33686–33697, 2019.

[25] H. Wymeersch, S. Marano, W. M. Gifford, and M. Z. Win, "A machine learning approach to ranging error mitigation for UWB localization," *IEEE Trans. Commun.*, vol. 60, no. 6, pp. 1719–1728, Jun. 2012.

[26] L. Schmid, D. Salido-Monzu, and A. Wieser, "Accuracy assessment and learned error mitigation of UWB ToF ranging," in *Proc. Int. Conf. Indoor Positioning Indoor Navigat. (IPIN)*, Sep. 2019, pp. 1–8.

[27] J. Sidorenko, V. Schatz, N. Scherer-Negenborn, M. Arens, and U. Hugentobler, "Error corrections for ultrawideband ranging," *IEEE Trans. Instrum. Meas.*, vol. 69, no. 11, pp. 9037–9047, Nov. 2020.

[28] J. Zhang, W. Wang, X. She, and X. Li, "2-D indoor passive real-time location system based on ultrawideband technology," *IEEE Trans. Instrum. Meas.*, vol. 71, pp. 1–17, 2022.

[29] S. Chen, D. Yin, and Y. Niu, "Research and implementation of improved SS-TWR TOA positioning method based on UWB," in *Proc. Int. Conf. Auto. Unmanned Syst. (ICAUS)*, 2021, pp. 3424–3434.

[30] D.-H. Kim, G.-R. Kwon, J.-Y. Pyun, and J.-W. Kim, "NLOS identification in UWB channel for indoor positioning," in *Proc. 15th IEEE Annu. Consum. Commun. Netw. Conf. (CCNC)*, Jan. 2018, pp. 1–4.

[31] C. Jiang, J. Shen, S. Chen, Y. Chen, D. Liu, and Y. Bo, "UWB NLOS/LOS classification using deep learning method," *IEEE Commun. Lett.*, vol. 24, no. 10, pp. 2226–2230, Oct. 2020.

[32] Z. Zeng, S. Liu, and L. Wang, "NLOS identification for UWB based on channel impulse response," in *Proc. 12th Int. Conf. Signal Process. Commun. Syst. (ICSPCS)*, Dec. 2018, pp. 1–6.

[33] K. Wen, K. Yu, and Y. Li, "NLOS identification and compensation for UWB ranging based on obstruction classification," in *Proc. 25th Eur. Signal Process. Conf. (EUSIPCO)*, Aug. 2017, pp. 2704–2708.

[34] Z. Zeng, S. Liu, and L. Wang, "UWB NLOS identification with feature combination selection based on genetic algorithm," in *Proc. IEEE Int. Conf. Consum. Electron. (ICCE)*, Jan. 2019, pp. 1–5.

[35] Z. Zeng, R. Bai, L. Wang, and S. Liu, "NLOS identification and mitigation based on CIR with particle filter," in *Proc. IEEE Wireless Commun. Netw. Conf. (WCNC)*, Apr. 2019, pp. 1–6.

[36] S. Angarano, V. Mazzia, F. Salvetti, G. Fantin, and M. Chiaberge, "Robust ultra-wideband range error mitigation with deep learning at the edge," *Eng. Appl. Artif. Intell.*, vol. 102, Jun. 2021, Art. no. 104278.

[37] K. Yu, K. Wen, Y. Li, S. Zhang, and K. Zhang, "A novel NLOS mitigation algorithm for UWB localization in harsh indoor environments," *IEEE Trans. Veh. Technol.*, vol. 68, no. 1, pp. 686–699, Jan. 2019.

[38] D.-H. Kim, A. Farhad, and J.-Y. Pyun, "UWB positioning system based on LSTM classification with mitigated NLOS effects," *IEEE Internet Things J.*, vol. 10, no. 2, pp. 1822–1835, Jan. 2023.

[39] *IEEE Standard for Low-Rate Wireless Networks–Amendment 1: Enhanced Ultra Wideband (UWB) Physical Layers (PHYs) and Associated Ranging Techniques*, IEEE Standard 802.15.4z-2020 (Amendment to IEEE Standard 802.15.4-2020), pp. 1–174, 2020.

[40] S. Monta, S. Promwong, and V. Kingsakda, "Evaluation of ultra wideband indoor localization with trilateration and min-max techniques," in *Proc. 13th Int. Conf. Electr. Eng./Electron., Comput., Telecommun. Inf. Technol. (ECTI-CON)*, Jun. 2016, pp. 1–4.

[41] W. Chantaweesomboon, C. Suwatthikul, S. Manatrinon, K. Athikulwongse, K. Kaemarungsi, R. Ranron, and P. Suksompong, "On performance study of UWB real time locating system," in *Proc. 7th Int. Conf. Inf. Commun. Technol. Embedded Syst. (IC-ICTES)*, Mar. 2016, pp. 19–24.

[42] H. Yin, W. Xia, Y. Zhang, and L. Shen, "UWB-based indoor high precision localization system with robust unscented Kalman filter," in *Proc. IEEE Int. Conf. Commun. Syst. (ICCS)*, Dec. 2016, pp. 1–6.

[43] A. Duru, E. Sehirli, and I. Kabalci, "Ultra-wideband positioning system using TWR and lateration methods," in *Proc. 4th Int. Conf. Eng. MIS*, 2018, pp. 1–4.

[44] J. J. Pérez-Solano, S. Ezpeleta, and J. M. Claver, "Indoor localization using time difference of arrival with UWB signals and unsynchronized devices," *Ad Hoc Netw.*, vol. 99, Mar. 2020, Art. no. 102067.

[45] N. Wang, X. Yuan, L. Ma, and X. Tian, "Research on indoor positioning technology based on UWB," in *Proc. Chin. Control Decis. Conf. (CCDC)*, Aug. 2020, pp. 2317–2322.

[46] B. Yan and L. Xiaochun, "Research on UWB indoor positioning based on TDOA technique," in *Proc. 9th Int. Conf. Electron. Meas. Instrum.*, Aug. 2009, pp. 1–167.

[47] T. Zhou and Y. Cheng, "Positioning algorithm of UWB based on TDOA technology in indoor environment," in *Proc. 11th Int. Conf. Inf. Technol. Med. Educ. (ITME)*, Nov. 2021, pp. 261–266.

[48] C.-D. Wann and C.-S. Hsueh, "NLOS mitigation with biased Kalman filters for range estimation in UWB systems," in *Proc. TENCON IEEE Region Conf.*, Oct. 2007, pp. 1–4.

[49] S. R. Jondhale, R. Maheswar, and J. Lloret, *Received Signal Strength Based Target Localization and Tracking Using Wireless Sensor Networks*. Berlin, Germany: Springer, 2022.

[50] S. R. Jondhale and R. S. Deshpande, "Tracking target with constant acceleration motion using Kalman filtering," in *Proc. Int. Conf. Adv. Commun. Comput. Technol. (ICACCT)*, Feb. 2018, pp. 581–587.

[51] C. Zhang, X. Bao, Q. Wei, Q. Ma, Y. Yang, and Q. Wang, "A Kalman filter for UWB positioning in LOS/NLOS scenarios," in *Proc. 4th Int. Conf. Ubiquitous Positioning, Indoor Navigat. Location Based Services (UPINLBS)*, Nov. 2016, pp. 73–78.

[52] Y.-M. Lu, J.-P. Sheu, and Y.-C. Kuo, "Deep learning for ultra-wideband indoor positioning," in *Proc. IEEE 32nd Annu. Int. Symp. Pers., Indoor Mobile Radio Commun. (PIMRC)*, Sep. 2021, pp. 1260–1266.

SANGMO SUNG received the M.S. degree from the Department of Electronic Engineering, Hanyang University, South Korea, in 2020, where he is currently pursuing the Ph.D. degree under the supervision of Prof. Jae-Il Jung. His research interests include modeling and performance enhancement of vehicular networks, throughput enhancement in vehicle communication, artificial intelligence algorithms, UWB-based data communication, indoor positioning, and UWB-based localization technologies.

HOKEUN KIM received the Ph.D. degree in EECS from UC Berkeley, in 2017, with a focus on IoT security. He is currently an Assistant Professor with the Department of Electronic Engineering, Hanyang University, Seoul, South Korea, and a Researcher with the Department of EECS, UC Berkeley. Before joining Hanyang University, he spent four years in the industry with Silicon Valley and continued research on the internet and cloud security with Google. His research interests include computer security, the IoT, real-time systems, cyber-physical systems, and computer architecture. He received the ACM/IEEE Best Paper Award and the IEEE Micro Top Picks Honorable Mention for his research contributions to IoT and computer architecture.

JAE-IL JUNG (Member, IEEE) received the B.S. degree in electronic engineering from Hanyang University, Seoul, South Korea, in 1981, the M.S. degree in electrical and electronic engineering from the Korea Advanced Institute of Science and Technology (KAIST), Seoul, in 1984, and the Ph.D. degree in computer science and networks from the Ecole Nationale Superieure des Telecommunications (ENST), Paris, France, in 1993. After receiving his M.S. degree, he was with the Telecommunication Network Research Laboratories, Korea Telecom, from 1984 to 1997. He is currently a Professor with Hanyang University. His research interests include wireless networks and autonomous vehicle technology.

• • •